journal

J. Am. Ceram. Soc., 1–6 (2012)
DOI: 10.1111/j.1551-2916.2012.05163.x

Influence of Ammonia on Properties of Nanocrystalline Barium Titanate Particles Prepared by a Hydrothermal Method

San Moon,[‡] Hyun-Wook Lee,[‡] Chang-Hak Choi,[§] and Do Kyung Kim[†,‡]

[‡]Department of Materials Science and Engineering, KAIST, Daejeon 305-701, Republic of Korea

[§]LCR Material Development Group, Samsung Electro-Mechanics, Suwon 443-743, Republic of Korea

The influence of ammonia on $BaTiO_3$ particles prepared via hydrothermal synthesis is discussed. Two kinds of Ti-precursors, amorphous (with ammonia) and anatase (without ammonia), are synthesized by a hydrolysis reaction using Ti-butoxide as the starting material. Amorphous Ti-precursors are found to be excellent for this purpose and offer several advantages over anatase. Superior tetragonal properties of $BaTiO_3$ powders with more uniform particle sizes can be achieved at 200°C after 24 h using amorphous Ti-precursors. X-ray photoelectron spectroscopy was carried out on both types of Ti-precursor, and a decrease in H_2O adsorption on the amorphous Ti-precursors is confirmed. It is considered that the reduction in H_2O adsorption on the Ti-precursors results from the shielding effects of ammonia and is attributed to a decreased formation of intragranular pores in the $BaTiO_3$ particles. These suggested mechanisms are clarified by the results of *in situ* transmission electron microscopy observations and density measurements of the hydrothermally synthesized $BaTiO_3$.

I. Introduction

BARIUM titanate ($BaTiO_3$), and especially the tetragonal phase, has been extensively used and studied for dielectric materials in multilayer ceramic capacitors (MLCCs) owing to its outstanding dielectric properties.[1–3] Advances in microelectronic packaging and communication technologies necessitate ultra-high-capacity MLCCs. As the dielectric layer of MLCCs becomes thinner, nano-sized $BaTiO_3$ powders with diameters of less than 100 nm become essential to produce MLCCs offering ultra-high capacity.[4–7]

Traditionally, $BaTiO_3$ nano-sized particles are produced by the solid-state reaction of $BaCO_3$ with TiO_2 at high temperature over 900°C,[8] but this method leads to the formation of $BaTiO_3$ particles with uncontrolled and irregular morphology. Nanoparticles are therefore synthesized by means of various wet chemical routes such as sol–gel processing,[9] the oxalate route,[10] homogeneous precipitation,[11] and hydrothermal methods.[12,13] Among various methods for synthesizing $BaTiO_3$, hydrothermal methods in particular have been utilized for commercial production due to the following advantages: (1) the temperature range required for this method not only reduces energy costs but improves the reactivity of the products, and (2) high-purity and single-phase oxides with superfine particle sizes, narrow particle size distribution, and good crystallinity can be achieved at a relatively fast rate.[14–21]

Crytallographic properties of $BaTiO_3$ directly affect the qualities of MLCCs.[17–19] The wet chemically synthesized $BaTiO_3$ particles show structural peculiarities that are closely connected to the considerable content of water that is incorporated in the perovskite lattice. The particles have intragranular pores that are formed by the concentration of migrating vacancies and water inside them and prevent an increase in dielectric properties.[17,18] In the firing process of MLCCs, intragranular pores preferentially accumulate at the inner electrodes, resulting in bloating, cracking, and delamination.[19] Consequently, the synthesis of $BaTiO_3$ powders with better crystallographic properties is important for MLCC performance.

To synthesize high tetragonal $BaTiO_3$ particles via a hydrothermal reaction, strongly alkaline conditions ($pH \geq 12$) are essential.[20] Generally, KOH, NaOH, and ammonia have been used as mineralizers to achieve suitable pH conditions.[21–23] In particular, ammonia has been preferred over KOH and NaOH due to its ease of removal. Ammonia is not incorporated into the oxide matrix, and residual ammonia in $BaTiO_3$ powders can simply be removed during drying at 100°C.[23] Furthermore, it is effective in limiting the leaching of barium from barium titanate powders.[24] However, the influence of ammonia on the hydrothermal synthesis of $BaTiO_3$ powders, over and above its effect in increasing the pH, has not been thoroughly explored to date.

In this work, we carried out surface analyses of two kinds of hydrolyzed Ti precursors to confirm other roles played by ammonia apart from its function as an alkaline mineralizer on the hydrothermal synthesis of $BaTiO_3$. To obtain structural information on the environment of the surface atoms and to determine the nature of the surface reactive groups, X-ray photoelectron spectroscopy (XPS) was carried out. XPS has been extensively used to not only investigate the interaction of water with TiO_2 in detail, but to obtain a better understanding of the TiO_2–water interface.[25–27] From such studies, it is postulated that different modes of interaction between H_2O and Ti-precursors result in dissimilar microstructures and densities of the $BaTiO_3$ particles, which are in turn investigated using *in- situ* transmission electron microscopy (TEM) and pycnometry, respectively.

II. Experimental Procedure

(1) Synthesis

Two kinds of Ti-precursor were prepared by the hydrolysis of Ti-butoxide ($Ti[O(CH_2)_3{\cdot}CH_3]_4$ (reagent grade 97%, Aldrich Chemical Co., Milwaukee, WI). The first sample, Ti-butoxide (0.025 mol), was diluted with 5 ml high-purity ethanol and 5 ml deionized water added to the solution. The second sample was prepared by a similar procedure except that 4 ml of ammonia solution was added to the mixed solution. The Ti-precursor powders were obtained for analysis by washing with deionized water and EtOH and drying at 80°C for 24 h in air.

E. Suvaci—contributing editor

Manuscript No. 30602. Received November 01, 2011; approved February 14, 2012.
[†]Author to whom correspondence should be addressed. e-mail: dkkim@kaist.ac.kr

For the preparation of $BaTiO_3$ powders, the above solutions were dispersed under magnetic stirring at 80°C, followed by the addition of 10 ml of an aqueous suspension of 37.5 M barium hydroxide monohydrate ($Ba(OH)_2 \cdot H_2O$, 98%, Aldrich Chemical Co.). Both final suspensions, which yielded a Ba:Ti molar ratio of 1.5:1, were transferred into a 100 ml Teflon-lined stainless-steel autoclave with a fill factor of 60%. The autoclaves were sealed and kept at 200°C for 24 h under autogenous pressure and then cooled to room temperature. The resultant products were filtered and washed with deionized water and EtOH several times, and subsequently dried at 80°C for 24 h in air.

(2) Characterization

The X-ray diffraction (XRD) data for Ti-precursors and $BaTiO_3$ powders were recorded on a diffractometer (Model D/MAM 2500, Rigaku Co., Tokyo, Japan), using Cu$K\alpha$ radiation ($\lambda = 1.5406$ Å) at 40 kV and 300 mA, and collected over a 2θ range of 20– 80°. The microstructures of the Ti-precursors were observed using field-emission transmission electron microscopy (FE–TEM) (Model JEM-3010, JEOL, Tokyo, Japan). The mean size and morphology of the $BaTiO_3$ particles were investigated by field-emission scanning electron microscopy (FE–SEM) (Model XL30, Philips, Amsterdam, the Netherlands). *In situ* microstructure evolution of the $BaTiO_3$ particles up to 500°C was observed using *in situ* TEM (Model JEM-3011, JEOL). For surface analysis of Ti-precursors, XPS (Model Sigma Probe, Thermo VG Scientific, Waltham, MA) was performed using Al Kα radiation under a vacuum of 1×10^{-10} Torr. The energy scale of the spectrometer was calibrated with pure Ag and Cu samples and the binding energies were measured with a precision of ±0.25 eV. Fourier-transform infrared spectroscopy (FT-IR) (Model IFS66V/S & HYPERION, Bruker Optiks, Billerica, MA) data for the $BaTiO_3$ powders were obtained using the KBr pellet technique. A commercial helium pycnometer (Model AccuPyc-1330, Micrometrics, Gosford, NSW, Australia) was used to measure the powder density of $BaTiO_3$ after annealing at temperatures in the range of 100°C–1100°C.

III. Results and Discussion

Figures 1(a) and (b) shows the XRD patterns of the as-synthesized Ti-precursors hydrolyzed from Ti-butoxide. The pH values of Ti-precursors hydrolyzed with and without ammonia solution are 10 and 4, respectively, and the addition of ammonia causes the formation of a different phase. By indexing the patterns in Fig. 1(a), the hydrolyzed products obtained without ammonia are consistent with the anatase structure (JCPDS No. 89-4921). As shown in Fig. 1(b), an amorphous phase was formed via the hydrolysis reaction with ammonia. The transformation from anatase to an amorphous phase with the addition of ammonia is presumably attributable to the alkaline conditions, which cause a breakage of Ti–O–Ti bonds.[28]

The XRD patterns of the $BaTiO_3$ powders, shown in Figs. 1(c) and (d), are well fitted to the peak positions of the standard tetragonal $BaTiO_3$ phase (JCPDS No. 05-0626). Normally, the diffraction pattern in the $2\theta = 45°$ region is characteristic of the presence of either a cubic or tetragonal $BaTiO_3$ structure. The tetragonal phase has two peaks, (002) and (200), which are clearly separated near $2\theta = 45°$. Only the (002) peak of the cubic phase, lying between two tetragonal phases, may overlap due to broadening of the peaks.[29] In the present case, the splitting of cubic (200) into tetragonal (200) and (002) reflections can be clearly observed. Accordingly, the synthesized $BaTiO_3$ phases indicate a tetragonal structure.

It has been widely reported that a solution with a high pH value is required to synthesize highly tetragonal $BaTiO_3$.[30–32] In our experiments, the pH of the two different Ti-precursors was approximately 4 (without ammonia) and 10 (with ammonia). However, after mixing with an aqueous solution of Ba $(OH)_2 \cdot H_2O$, the pH values of both seed $BaTiO_3$ suspensions were around 13. Hence, the experimental conditions were sufficient for the synthesis of $BaTiO_3$ according to the stability

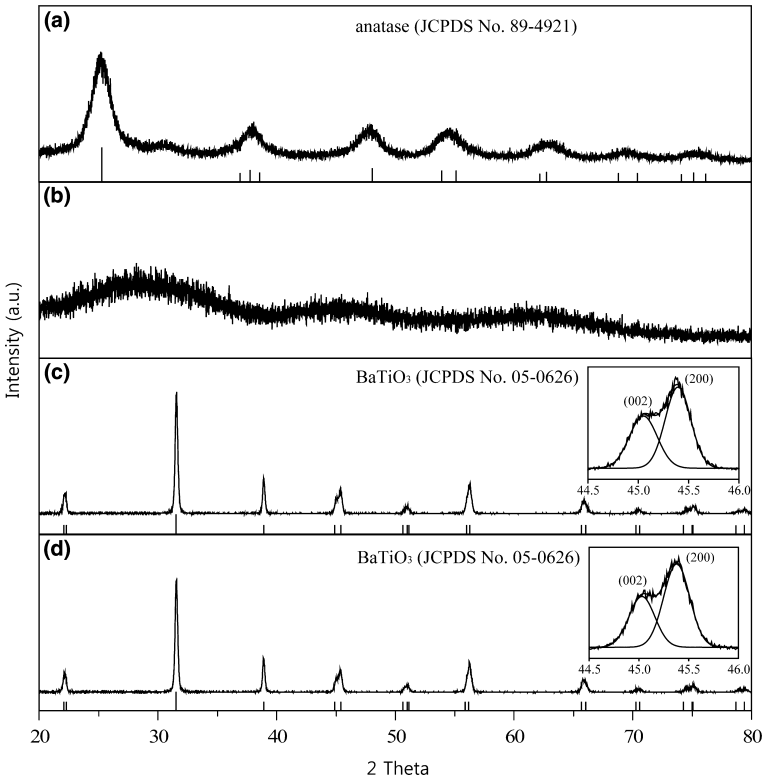

Fig. 1. X-ray diffraction patterns of (a) Ti-precursors synthesized without ammonia and (b) with ammonia, and (c) $BaTiO_3$ synthesized without ammonia and (d) with ammonia. The insets in (c) and (d) show the peak splitting of (002) and (200).

diagram.[32] To demonstrate the tetragonality, c/a, for the as-synthesized $BaTiO_3$ powders, we performed Rietveld refinement. The initial Rietveld refinement was carried out by the zero-point shift, the unit-cell, and background parameters. After a good match of the peak positions was achieved, the peak profile parameters including the peak asymmetry were refined. Based on this approach, the final tetragonalities, which were averaged over 10 times for $BaTiO_3$ powders synthesized with and without ammonia, were 1.0076 and 1.0071, respectively. In spite of the similar pH values of the seed $BaTiO_3$ suspensions, hydrothermally synthesized $BaTiO_3$ powders with ammonia have higher tetragonality. Therefore, it can be concluded that the characteristics of ammonia other than its effect on pH accounted for the differences in tetragonality parameters under a sufficiently high pH condition. This aspect is discussed further in the following sections.

TEM and SEM analyses were carried out to investigate the microstructures of the nanocrystals. Figures 2(a) and (b) shows typical TEM images of the Ti-precursors, hydrolyzed without and with ammonia solution, respectively. The morphologies of the two precursors are similar to those of highly agglomerated particles of diameters of less than 10 nm. However, the final $BaTiO_3$ products synthesized via a hydrothermal reaction possess some different characteristics, as illustrated by the SEM images in Figs. 2(c) and (d). The average particle sizes (*ca.* 95 nm) of $BaTiO_3$ derived from the anatase Ti-precursors were higher than those of the $BaTiO_3$ particles (*ca.* 85 nm) obtained from the amorphous precursors. In addition, the particle size and morphology of $BaTiO_3$ powders synthesized with ammonia were more uniform. The dispersity (D_{SEM99}/D_{SEM50}) of the final $BaTiO_3$ powders synthesized without and with ammonia was 2.13 and 1.62, respectively. Kutty *et al.* suggested that amorphous Ti-precursors provide the fastest reaction, and anatase with rutile, the slowest.[33] Furthermore, whereas abundant nucleation sites are present in the amorphous Ti-precursor reaction, nucleation occurs only at the interface between the solution and the smallest anatase particles, resulting in a larger average $BaTiO_3$ particle size.[34] Consequently, it is proposed that the more uniform and smaller particle sizes of $BaTiO_3$ synthesized from the amorphous Ti-precursors are likely to be due to the influence of ammonia, which controls the reactivity of the precursors.

To further discuss the influence of ammonia on the surface of the Ti-precursors, the XPS data are considered. Figures 3(a) and (b) shows the O 1*s* spectra of anatase and amorphous Ti-precursors, revealing four components at 529.7, 531.0, 532.2, and 533.5 eV. The major contribution arises from the bulk O^{2-} atoms with a binding energy of 529.7 eV, which is the value usually reported for TiO_2 samples.[35] The two other components (531.0 and 532.2 eV) can be assigned to the two-fold and single-fold oxygen atoms, respectively.[26,36,37] Finally, the peak at 533.5 eV can be tentatively assigned to the oxygen of molecular physisorbed water molecules in the upper hydration layer. Three kinds of oxygen atoms could be present on the TiO_2 surface: three-fold near-surface oxygen atoms (denoted O_s) that are almost identical to the bulk atoms (529.7 eV); two-fold atoms,

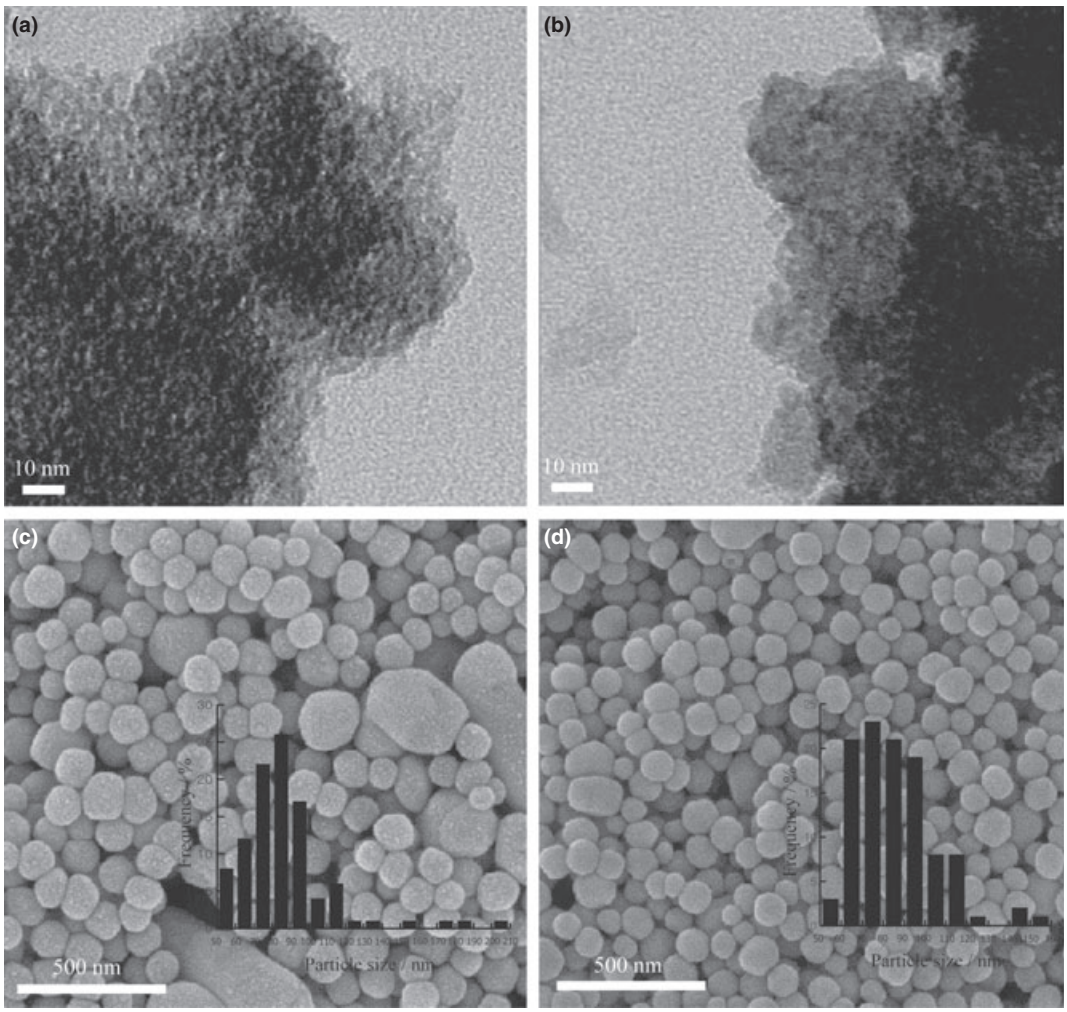

Fig. 2. TEM images of (a) Ti-precursors synthesized without ammonia (anatase) and (b) with ammonia (amorphous), and SEM images of (c) $BaTiO_3$ synthesized by using anatase and (d) amorphous Ti-precursors as Ti seeds. Both Ti-precursor particles are highly agglomerated and appear similar. $BaTiO_3$ synthesized with ammonia has more uniform particles.

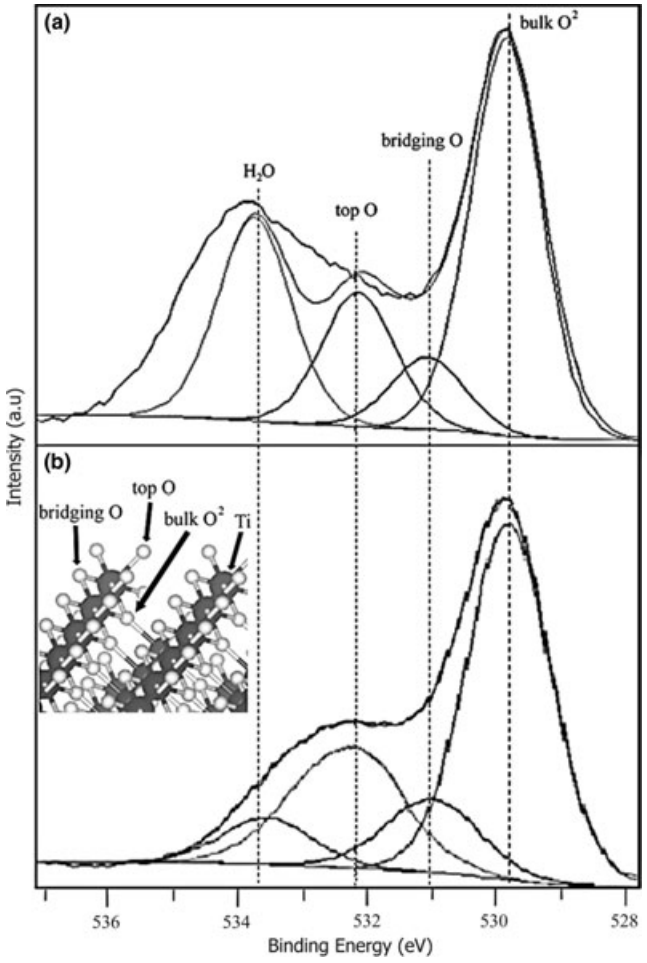

Fig. 3. O 1*s* spectra of (a) anatase and (b) amorphous Ti-precursors. Surface oxygen peaks of amorphous Ti-precursors are of higher intensity than those of anatase Ti-precursors. The inset in (b) shows the dry TiO_2 (100) face. Bridging O (531.0 eV) and top O (532.2 eV) change in abundance from 19.6% to 21.8% and from 34.7% to 45.5%, respectively, with ammonia. The adsorbed H_2O peak (533.5 eV) is reduced from 63.0% to 14.6%.

referred to as "bridging" oxygen atoms (531.0 eV); and single-fold atoms, denoted as "top" oxygen (532.2 eV).[35] Table I shows the relative areas of each peak, revealing that the surface oxygen peaks of Ti-precursors synthesized with ammonia (531.0 eV: 21.8% and 532.2 eV: 45.5%) were of higher intensity than those of Ti-precursors synthesized without ammonia (531.0 eV: 19.6% and 532.2 eV: 34.7%). It was previously reported that some of the Ti–O–Ti bonds might be broken in alkaline solution.[28] Consistent with this finding, it is suggested that the larger quantity of surface oxygen in the present study results from the rupture of such bonds under the high pH conditions used. The XPS results are consistent with the proposed difference in nucleation sites densities between the amorphous and anatase Ti-precursors mentioned above. Therefore, it is speculated that the increase

Table I. Characteristics of O (1*s*) Peaks on XPS Spectrum of TiO_2

Binding energy ±0.2 (eV)	Oxygen surface groups	Anatase (%)	Amorphous (%)
529.7	Os	100	100
531.0	Bridging O group	19.6	21.8
532.2	Top O group	34.7	45.5
533.5	H_2O in upper layer	63.0	14.6

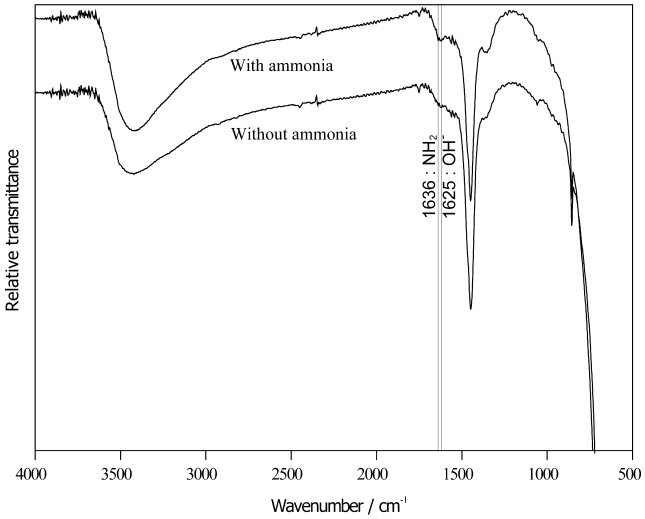

Fig. 4. FT-IR spectra of $BaTiO_3$ synthesized by using anatase (without ammonia) and (d) amorphous Ti-precursors (with ammonia) as Ti seeds. The $BaTiO_3$ synthesized with amorphous Ti-precursors only shows the NH_2 peaks in IR spectra. The NH_2 absorbed on $BaTiO_3$ has a hydrophobic tail, shielding the surface from H_2O adsorption during the hydrothermal reaction.

in reactive areas of Ti-precursors with Ba^{2+} can be attributed to the addition of ammonia, which caused a faster and more uniform reaction between these two entities.

Another notable feature in the XPS spectra is the lower intensity of the H_2O peak in the amorphous Ti-precursors. The H_2O absorbed on TiO_2 dissociates to OH^- on titanium atoms and H^+ on oxygen atoms, and other water molecules undergo hydrogen bonding with the dissociated H^+.[38,39] It is suggested that the amounts of dissociated H_2O and H_2O molecules on Ti-precursors may affect the amount of water incorporated into the perovskite lattice of $BaTiO_3$ as hydroxyl groups during the hydrothermal synthesis. Corresponding to the substantial quantity of OH^- ions, a large amount of protons existed in the oxygen sublattice of $BaTiO_3$. The protons on the O sites of hydrothermally synthesized $BaTiO_3$ particles must be compensated by the simultaneous formation of barium and titanium vacancies.[19] Moreover, the presence of OH^- in the structure would cause an internal stress that is expected to hinder the transformation from cubic to tetragonal structures and that effectively stabilizes cubic $BaTiO_3$ at room temperature.[40] It is further suggested that the higher tetragonality of $BaTiO_3$ particles synthesized with ammonia can be attributed to the smaller concentration of defects resulting from the smaller amount of adsorbed H_2O on the Ti-precursors.

This hypothesis was tested by investigating the activation of ammonia on Ti-precursors. The FT-IR bands at 1625 and 1636 cm^{-1} (Fig. 4) showed the presence of OH^- and NH_2 stretching vibrations in the as-synthesized $BaTiO_3$ powders, respectively. Both FTIR spectra show bands at 1625 cm^{-1}. However, the bands of coordinated NH_2 (1636 cm^{-1}) are clearly evident only in the spectrum of $BaTiO_3$ synthesized with ammonia. From previous research based on the adsorption of H_2O and NH_3 on TiO_2, it was reported that H_2O and NH_3 were adsorbed on the same site (Ti atoms) and that the adsorption energy of NH_3 was substantially lower than that of H_2O (adsorption energy of dissociated H_2O: −34.78 kcal/mol, molecular H_2O: −18 kcal/mol, and molecular NH_3: −92.64, −84.35 kcal/mol).[39] It is widely accepted that NH_3 adsorbed on TiO_2 is easily transformed to amide NH_2 species with a long hydrophobic tail by hydrogen abstraction.[41–43] In agreement with findings reported elsewhere, it can be speculated that NH_2 with a hydrophobic tail hinders the adsorption of H_2O on the Ti-precursors during the hydrothermal reaction to $BaTiO_3$, and might result in a

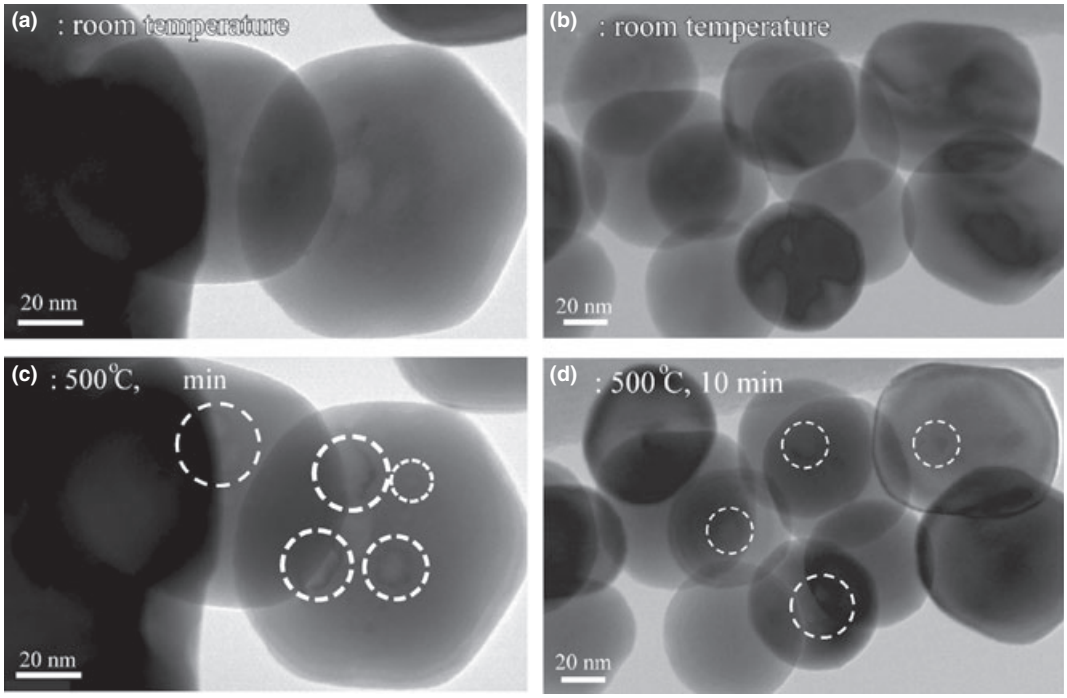

Fig. 5. *In situ* TEM images of $BaTiO_3$ synthesized by using anatase Ti-precursors at 25°C (a) and 500°C (c) and by using amorphous Ti-precursors at 25°C (b) and 500°C (d). With an increase in temperature, the intragranular pores (white circles) in the $BaTiO_3$ particles appear. The pores in $BaTiO_3$ particles synthesized by using anatase are more easily observed.

smaller concentration of defects and higher tetragonality of $BaTiO_3$ particles synthesized with ammonia.

Figure 5 shows TEM images of $BaTiO_3$ particles at 25 and 500°C obtained by *in situ* TEM. The TEM images at 25°C illustrate $BaTiO_3$ particles without intragranular pores. However, pores could be observed after heating to 500°C. When the $BaTiO_3$ particles were heated to 500°C, the volume of point defects, which were not previously visible, accumulates to form fine pores that are easily detectable via TEM.[19] The notable difference is that the as-synthesized $BaTiO_3$ particles produced without ammonia showed a larger population of intragranular pores than the as-synthesized $BaTiO_3$ particles obtained with ammonia after heating to 500°C. This finding is consistent with the XPS analysis, revealing that the lattice defects of $BaTiO_3$ particles derived from amorphous Ti-precursors show a decrease in number due to the smaller quantity of H_2O adsorbed on the Ti-precursors.

Finally, the density measurements are considered because they can be used to characterize the intragranular porous nature of the $BaTiO_3$ powders. Figure 6 shows the density variation of the $BaTiO_3$ samples, which were heated for 2 h in a temperature range of 100°C–1100°C. Pycnometry revealed that the densities of $BaTiO_3$ synthesized with ammonia were higher than those of $BaTiO_3$ synthesized without ammonia up to heating temperatures of ~700°C. According to the *in situ* TEM results, the intragranular pores were visible at 500°C. Therefore, the higher densities of $BaTiO_3$ synthesized with ammonia at ~500°C and 500°C–700°C can be readily explained in terms of fewer point defects and a lower intragranular porosity, with the latter resulting from the accumulation of such defects. The increase in densities, approaching the normal theoretical density in the temperature range of 700°C–1100°C, resulted from significant grain growth, which is most likely stimulated by an Ostwald ripening mechanism and the release of intragranular pores.[19] Consequently, based on a combination of XPS, *in situ* TEM, and pycnometer results, it is suggested that the decreases in point defect abundance and intragranular porosity in the $BaTiO_3$ particles are attributable to a reduction in H_2O adsorption on Ti-precursors, which are shielded from H_2O via the adsorbed ammonia during the hydrothermal synthesis of

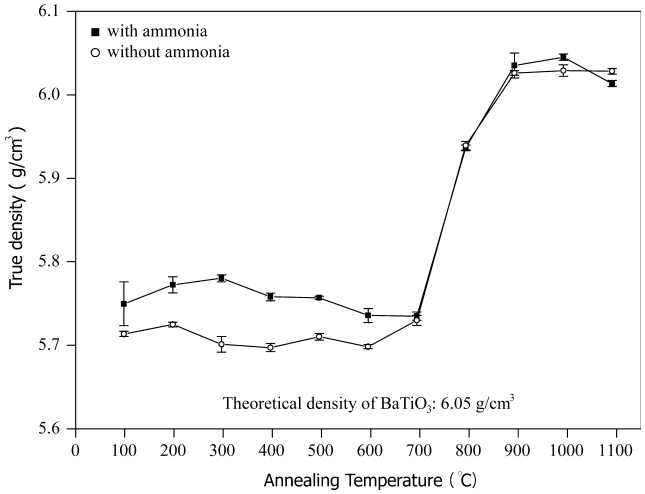

Fig. 6. Measured density of $BaTiO_3$ heat-treated at temperatures in the range 100°C–1100°C for 2 h. Up to 700°C, the densities of $BaTiO_3$ from amorphous Ti-precursors are higher. The hydrophobic tails of NH_2 entities adsorbed on $BaTiO_3$ prevents the formation of inner pores. Both $BaTiO_3$ products have an ideal density over 900°C, which results from the disappearance of pores.

$BaTiO_3$. Therefore, superior tetragonal $BaTiO_3$ powders with uniform morphology and particle sizes could be obtained under similar pH conditions in the case of ammonia addition.

IV. Conclusion

Ammonia plays a crucial role in the hydrothermal synthesis of $BaTiO_3$ powders and leads to smaller particle sizes, a narrower size distribution, and higher tetragonality. The size properties are ascribed to the amorphous Ti-precursors hydrolyzed with ammonia having a larger reactive surface area, thereby allowing fast and uniform reaction with the Ba source. Higher tetragonality is due to the adsorbed NH_2 entities on the Ti-precursors, which are shielded from H_2O

absorption. The reduction in the quantity of absorbed H_2O on the Ti-precursors results in a decrease in the concentration of point defects in the $BaTiO_3$ particles, which in turn suppresses the formation of intragranular pores at high temperature.

The experimental results confirmed that the high tetragonality of $BaTiO_3$ can be attributed to the influence of ammonia, not only in increasing the pH value of solution but in decreasing the concentration of point defects. The combined effects of ammonia lead to better properties of hydrothermally synthesized $BaTiO_3$ particles for application in MLCCs.

Acknowledgments

This work was supported by the Samsung Electro-Mechanics Co. Ltd. through the Center for Advanced MLCC-Manufacturing Processes, Korea Science and Engineering Foundation (KOSEF) grant (NO. R01-2008-000-20480-0), the National Research Foundation of Korea (NRF) funded by the Ministry of Education, Science and Technology (MEST) (NRF-2010-C1AAA001-2010-0029031), and the Priority Research Centers Program through the NRF funded by MEST (2009-0094041).

References

[1]B. Huybrechts, K. Ishizaki, and M. Takata, "The Positive Temperature Coefficient of Resistivity in Barium Titanate," *J. Mater. Sci.*, **30**, 2463–74 (1995).

[2]G. J. Choi, S. K. Lee, K. J. Woo, K. K. Koo, and Y. S. Cho, "Characteristics of $BaTiO_3$ Particles Prepared by Spray-Coprecipitation Method Using Titanium Acylate-Based Precursors," *Chem. Mater.*, **10**, 4104–13 (1998).

[3]M. Z. C. Hu, G. A. Miller, E. A. Payznt, and C. J. Rawn, "Homogeneous (Co)Precipitation of Inorganic Salts for Synthesis of Monodispersed Baium Titanate Particles," *J. Mater. Sci.*, **35**, 2927–36 (2000).

[4]G. Arlt, D. Hennings, and G. De With, "Dielectric Properties of Fine-Grained Barium Titanate Ceramics," *J. Appl. Phys.*, **58**, 1619–25 (1985).

[5]K. Ishikawa, K. Yoshikawa, and N. Okada, "Size Effect on the Ferroelectric Phase Transition in $PbTiO_3$ Ultrafine Particles," *Phys Rev. B*, **37**, 5852–5 (1988).

[6]K. Uchino, E. Sadanaga, and T. Hirose, "Dependence of the Crystal Structure on Particles Size in Barium Titanate," *J. Am. Ceram. Soc.*, **72**, 1555–8 (1989).

[7]M. H. Frey and D. A. Payne, "Grain-Size Effect on Structure and Phase Transformation for Barium Titanate," *Phys. Rev. B*, **54**, 3158–68 (1996).

[8]G. Spieb, "Uber die bildung von bariummetatitanat," *Ber. Dtsch. Keram. Ges.*, **38**, 495–528 (1961).

[9]H. Shimooka and M. Juwabara, "Crystallinity and Stoichiometry of Nano-Structured Sol-Gel Derived $BaTiO_3$ Monolithic Gels," *J. Am. Ceram. Soc.*, **79**, 2983–5 (1996).

[10]H. I. Hsiang and F. S. Yen, "Effect of Crystalline Size on the Ferroelectric Domain Growth of Ultrafine BaTiO3 Powders," *J. Am. Ceram. Soc.*, **79**, 1053 –60 (1996).

[11]M. Stockenhuber, H. Mayer, and J. A. Lercher, "Preparation of Barium Titanates from Oxalates," *J. Am. Ceram. Soc.*, **76**, 1185–90 (1993).

[12]K.-Y. Chen and Y.-W. Chen, "Preparation of Barium Titanate Ultrafine Particles from Rutile Titania by a Hydrothermal Conversion," *Mater. Lett.*, **59**, 3543–9 (2005).

[13]M. Z.-C. Hu, V. Kurian, E. Andrew Payzant, C. J. Rawn, and R. D. Hunt, "Wet-Chemical Synthesis of Monodispersed Barium Titanate Particles – Hydrothermal Conversion of TiO_2 Microspheres to Nanocrystalline $BaTiO_3$," *Powder. Tech.*, **110**, 2–14 (2000).

[14]W. J. Dawson, "Hydrothermal Synthesis of Advanced Ceramic Powder," *J. Am. Ceram. Soc. Bull.*, **67**, 1673–8 (1988).

[15]S. B. Cho, B. Sridhar, and J. H. Adair, "Morpholgical Forms of α–Alumina Particles Synthesized in 1,4-Butanediol Solution," *J. Am. Ceram. Soc.*, **79**, 88–96 (1996).

[16]J. Moon, E. Suvaci, A. Morrone, S. A. Costantino, and J. H. Adair, "Formation Mechanisms and Morphological Changes During the Hydrothermal Synthesis of $BaTiO_3$ Particles from a Chemically Modified, Amorphous Titanium (hydrous) Oxide Precursor," *J. Eur. Ceram. Soc.*, **23**, 2153–61 (2003).

[17]D. Hennigs and S. Schreinemacher, "Characterization of Hydrothermal Barium Titanate," *J. Eur. Ceram. Soc.*, **9**, 41–6 (1992).

[18]Y. Yamashita, H. Yamamoto, and Y. Sakabe, "Dielectric Properties of BaTiO3 Thim Films Derived from Clear Emulsion of Well-Dispersed Nanosized $BaTiO_3$ Particles," *Jap. J. Appl. Phys.*, **43**, 6521–4 (2004).

[19]D. F. K. Hennings, C. Metzmacher, and B. Seriyati Schreinenacher, "Defect Chemistry and Microstructure of Hydrothermal Barium Titanate," *J. Am. Ceram. Soc.*, **84**, 179–82 (2001).

[20]M. M. Lencka and R. E. Riman, "Thermodynamic Modeling of Hydrothermal Synthesis of Ceramic Powders," *Chem. Mater.*, **5**, 61–70 (1993).

[21]S. K. Lee, T. J. Park, G. J. Choi, K. K. Koo, and S. Woo Kim, "Effects of KOH/BaTi and Ba/Ti Ratio on Synthesis of $BaTiO_3$ Powder by Coprecipitation/Hydrothermal Reaction," *Mater. Chem. Phys.*, **82**, 742–9 (2003).

[22]S.-K. Lee, G.-J. Choi, U.-Y. Hwang, K.-K. Koo, and T.-J. Park, "Effect of Molar Ration of KOH to Ti-isopropoxide on the Formation of $BaTiO_3$ Powders by Hydrothermal Method," *Mater. Lett.*, **57**, 2201–7 (2003).

[23]S. K. Tripathy, T. Sahoo, M. Mpjapatra, S. Anand, and R. P. Das, "XRD Studies on Hydrothermal Synthesized $BaTiO_3$ from TiO_2-$Ba(OH)_2$-NH_3 System," *Mater. Lett.*, **59**, 3543–9 (2005).

[24]W. Lu, M. Quilitz, and H. Schmidt, "Nanoscaled BaTiO3 Powders with a Large Surface Area Synthesized by Precipitation from Aqueous Solution: Preparation, Characterization and Sintering," *J. Eur. Ceram. Soc.*, **27**, 3149–59 (2007).

[25]L. Q. Wang, D. R. Baer, M. H. Engelhard, and A. N. Shultz, "The Adsorption of Liquid and Vapor Water on TiO_2(110) Surfaces: the Fole of Defects," *Surf. Sci.*, **344**, 237–50 (1995).

[26]R. L. Kurtz, R. Stockbauer, T. E. Madey, E. Roman, and J. L. De Segovia, "Synchrotron Radiation Studies of H_2O Adsorption on TiO_2, (110)," *Surf. Sci.*, **218**, 178–200 (1989).

[27]H. Perron, C. Domain, J. Roques, R. Drot, E. Simoni, and H. Catalette, "Periodic Density Functional Theory Investigation of the Uranyl Ion Sorption on the TiO_2 Rutile (110) Face," *Inorg. Chem.*, **45**, 6568–70 (2006).

[28]Z. Yuanm and B.-L. Su, "Titanium Oxide Nanotubes, Nanofibers and Nanowires," *Col. Surf. A*, **241**, 173–83 (2004).

[29]Y.-I. Kim, J. Kap Jung, and K.-S. Ryu, "Structural Study of Nano $BaTiO_3$ Powder by Rietveld Refinement," *Mater. Res. Bull.*, **39**, 1045–53 (2004).

[30]B. I. Lee, X. Wang, S. Joon Kwon, H. Maie, R. Kota, J. H. Hwang, J. G. Park, and M. Hu, "Synthesis of High Tetragonality Nanoparticle $BaTiO_3$," *Microelec. Eng.*, **83**, 463–70 (2006)

[31]H. Xu, L. Gao, and J. Guo, "Preparation and Characterization of Tetragonal Barium Titanate Powders by Hydrothermal Method," *J. Eur. Ceram. Soc.*, **22**, 1163–70 (2002).

[32]M. M. Lencka, and R. E. Riman, "Thernodynamic Modeling of Hydrothermal Synthesis of Ceramic Powder," *Chem. Mater.*, **5**, 61–70 (1993).

[33]R. Vivekanandan and T. R. N. Kutty, "Characterization of Barium Titanate Fine Powders Formed From Hydrothermal Crystalllization," *Powder. Tech.*, **57**, 181–92 (1989).

[34]J. A. Kerchner, J. Moon, R. E. Chodelka, A. A. Morrone, and J. H. Adair, "Nucleation and Formatation Mechanisms of Hydrothermally Derived Barium Titanate," *ACS Symp. Ser.*, **681**, 106–19 (1998).

[35]H. Perron, J. Vandenborre, C. Domain, R. Drot, J. Roques, E. Simoni, J.-J. Ehrhardt, and H. Catalette, "Combined Investigation of Water Sorption on TiO_2 Rutile (001) Single Crystal Face: XPS vs. Periodic DFT," *Surf. Sci.*, **601**, 518–27 (2007).

[36]W. Gopel, J. A. Anderson, D. Frankel, M. Jaehnig, K. Phillips, J. A. Schafer, and G. Rocker, "Surface Defects of TiO_2 (001): A conbined XPS, XAES and ELS study," *Surf. Sci.*, **139**, 333–46 (1984).

[37]T. K. Sham and M. S. Lazarus, "X-ray Photoelectron Spectroscopy Studies of Clean and Hydrated TiO_2 (Rutile) Surfaces," *Chem. Phys. Lett.*, **68**, 426 –32 (1979).

[38]T. Bredzona, G. Puchkovska, V. Shymanovska, J. Baran, and H. Ratajczak, "IR-Analysis of H-Bonded H_2O on the Pure TiO_2 Surface," *J. Mol. Struct.*, **700**, 175–81 (2004).

[39]I. Onal, S. Soyer, and S. Senkan, "Adsorption of Water and Ammonia on TiO_2-anatase Cluster Models," *Surf. Sci.*, **600**, 2457–69 (2006).

[40]F.-S. Yen, H.-I. Hsiang, and Y.-H. Chang, "Cubic to Tetragonal Phase Transformation of Ultrafine $BaTiO_3$ Crystalllites at Room Temperature," *Jpn. J. Appl. Phys.*, **34**, 6149–55 (1995).

[41]G. Ramis, L. Yi, G. Busca, M. Turco, E. Kotur, and R. J. Willey, "Adsortpion, Activation and Oxidation of Ammonia over SCR Catalysts," *J. Catal.*, **157**, 523–35 (1995).

[42]G. Ramis, L. Yi, and G. Busca, "Ammonia Activation Over Catalysts for the Selectibe Catalytic Reduction of NO_x and the Selective Catalytic Oxidation of NH_3. An FT-IR Study," *Catal. Today*, **28**, 373–80 (1996).

[43]G. Busca, L. Lietti, G. Ramis, and F. Berti, "Chemical and Mechanistic Aspects of the Selective Catalytic Reduction of NO_x by Ammonia Over Oxide Catalysts: A Review," *Appl. Catal. B: Environ.*, **18**, 1–36 (1998). □